BRAIN IMAGES SEGMENTATION BY OPTIMIZING CLUSTERING OF CONVOLUTION BASED FEATURES

Ronak Rafiq[1] ,Vikas Kumar [2]
M.Tech Scholar[1], Assistant Professor[2]
Galaxy Global Group Of Institutions
Ambala-Haryana , INDIA

Abstract- Brain tumor segmentation aims to separate the different tumor tissues such as active cells, necrotic core, and edema from normal brain tissues of White Matter (WM), Gray Matter (GM), and Cerebrospinal Fluid (CSF). MRI based brain tumor segmentation studies are attracting more and more attention in recent years due to non-invasive imaging and good soft tissue contrast of Magnetic Resonance Imaging (MRI) images. With the development of almost two decades, the innovative approaches applying computer-aided techniques for segmenting brain tumor are becoming more and more mature and coming closer to routine clinical applications. The purpose of this paper is to provide a comprehensive overview for MRI-based brain tumor segmentation methods. Firstly, a brief introduction to brain tumors and imaging modalities of brain tumors is given. In thesis proposed convolution based optimization. These step wise step refine the segmentation and improve the classification parameter with the help of particle swarm optimization.

Keywords: Magnetic Resonance Imaging, Gray Matter, White Matter, Cerebrospinal Fluid.

I. INTRODUCTION

Brain region segmentation or skull stripping is an essential step in neuroimaging application such as surgical, surface reconstruction, image registration etc. [1] [3]. The accuracy of all existing methods depends on the registration and image geometry. When this fails, the probability of success is very less. In order to avoid this, Convolutional Neural Network (CNN) is used. For brain extraction which is free from geometry and registration. CNN learned the connectedness and shape of the brain. Accurate diagnosis in medical procedure has attained using different imaging modalities such as Magnetic Resonance(MR) imaging, Computed Tomography (CT), digital mammography etc [8] [10]. These can provide very detailed and informative anatomy of a subject. Research community develops many methods. Deep learning, called as deep structured learning is one of the machine learning algorithms. It learns data from the input image using either supervised or unsupervised [4] [13]. There has been a significant effort in developing classical machine learning algorithms for segmentation of normal (e.g., white matter and gray matter) and abnormal brain tissues (e.g. Brain tumours). However, creation of the imaging features that enable such segmentation requires careful engineering and specific expertise. Furthermore, traditional machine learning algorithms do not generalize well [14] [15]. Despite a significant effort from the medical imaging research community, automated segmentation of the brain structures and detection of the abnormalities remain an unsolved problem due to normal anatomical variations in brain morphology, variations in acquisition settings and MRI scanners, image acquisition imperfections, and variations in the appearance of pathology. An emerging machine learning technique referred to as deep learning can help avoid limitations of classical machine learning algorithms, and its self-learning of features may enable identification of new useful imaging features for quantitative analysis of brain [12]. Deep learning techniques are gaining popularity in many areas of medical image analysis such as computer-aided detection of breast lesions, computer-aided diagnosis of breast lesions and pulmonary nodules, and in histopathological diagnosis.

1.1 Brain Region Segmentation

Brain tissue classification or segmentation is used for detection and diagnosis of normal and pathological tissues such as MS tissue abnormalities and tumors. These abnormalities could be identified by tracking of changes in volume, shape and regional distribution of brain tissue during follow-up of patients. Medical image segmentation is an essential step for most subsequent image analysis tasks. The segmentation of anatomic structure in the brain plays a crucial role in Nero imaging analysis. Successful numerical algorithms can help researchers, physicians and neurosurgeons to investigate and diagnose the structure and function of the brain in both health and disease. This has motivated the need for segmentation techniques that are robust in application involving abroad range of anatomic structure, disease and image type. The process of partitioning a digital image into multiple regions or sets of pixels is called image segmentation. Actually, partitions are different objects in image which have the same texture or colour. The result of image segmentation is a set of regions that collectively cover the entire image, or a set of contours extracted from the image [2] [6] [18].

1.2 Brain Segmentation Approaches

The details of Approaches as follows:

A. Edge based Technique for Brain Image Segmentation: Edge detection techniques transform images to edge images benefiting from the changes of grey tones in the images. As a result of this transformation, edge image is obtained without encountering any changes in physical qualities of the main image [18].

(a) ACO Approach: The ACO-based image edge detection approach aims to utilize a number of ants to move on a 2-D image for constructing a pheromone matrix, which represents the edge information at each pixel location of the image [18]. The proposed approach starts from the initialization process, and then runs for N iterations to

construct the pheromone matrix by iteratively performing both the construction process and the update process. Finally, the decision process is performed to determine the edge.

(b) Fuzzy Logic Approach: Cristiano Jacques Miosso and Adolfo Bauchspiess evaluated the performance of a fuzzy inference system (FIS) in edge detection. It was concluded that despite the much superior computational effort when compared to the Sobel operator, the FIS system presents greater robustness to contrast and lighting variations, besides avoiding obtaining double edges [18]

(c) GA Approach: GAs are robust in that they are not affected by spurious local optima in the solution space. This robustness is backed up by a strong mathematical foundation. Most interesting genetic application in edge detection is by Gudmundsson et al. [17] and is as described below. Edges are represented in a binary image, where each pixel takes on either the value zero (off) for a non-edge pixel or one (on) for an edge pixel. Each pixel in the binary map corresponds to an underlying pixel in the original image. This edge representation is simple, allows direct illustration of results, location of edge points maps directly onto the original image and, adjacency and orientation are preserved. By using the edge map as a solution space for the GA, no special mappings are required, small neighbourhood windows can be overlaid, and edge structures and pixels can be modified on a local, intuitive basis.

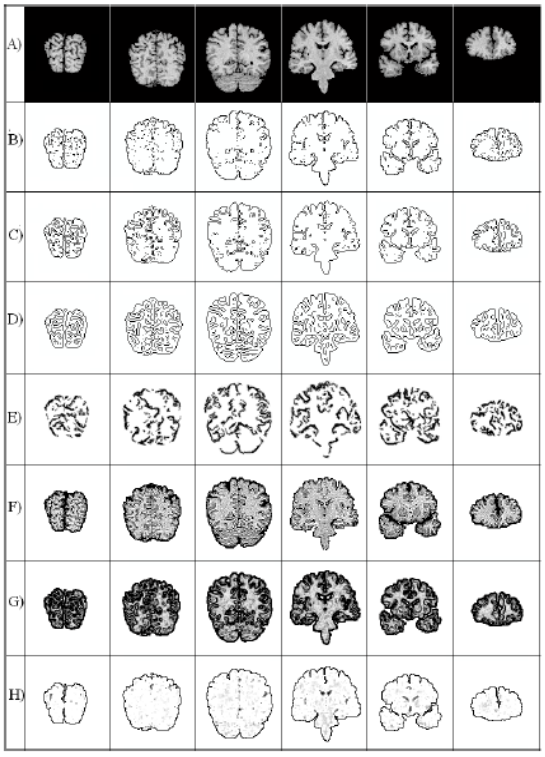

Figure 1.1: Edge based technique for brain image segmentation, a) Original images, b) using Prewitt method, c) using Roberts method, d) using Sobel method, e) using ACO method, f) using Fuzzy logic, g) using GA, h) using Neural Network [3]

(d) Neural Network Approach: Neural networks have been applied in many image segmentation problems like edge detection. There are many image based edge detection algorithms using neural networks, the most successful system was introduced by Rowley et al. [6]. The neural network technique in this section is such an approach, and functions just like a pattern classifier, which collects the input features and outputs the decisions [18].

B. Splite and Merge Technique for Brain Image Segmentation:

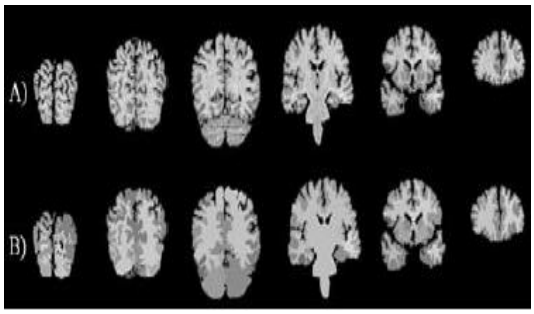

Figure 1.2: Using Splite and Merge algorithm for brain image segmentation

One of the basic properties of segmentation is the existence of a predicate which measures the region homogeneity. If this predicate is not satisfied for some region.On the other hand, if the predicate is satisfied for the union of two adjacent regions, then these regions are collectively homogeneous and should be merged into a single region. A method towards the satisfaction of these homogeneity criteria is the split-and-merge algorithm [5] [6]. Figure 2 shows the example image using splite and merge algorithm for brain image segmentation.

C. Hybrid Method for Brain Image Segmentation: A hybrid method is using granular rough sets for brain image segmentation. Recently, rough set theory has become a popular mathematical framework for granular computing and is used as a mathematical tool to analyse vagueness and uncertainty inherent in making decisions. The focus of rough set theory is on the ambiguity caused by limited discernibility of objects in the domain of discourse.

1.3 Deep Learning

Deep learning refers to neural networks with many layers (usually more than five) that extract a hierarchy of features from raw input images. It is a new and popular type of machine learning techniques that extract a complex hierarchy of features from images due to their self-learning ability as opposed to the hand-crafted feature extraction in classical machine learning algorithms. They achieve impressive results and generalizability by training on large amount of data. This allowed training of deep learning algorithms with millions of images and provided robustness to variations in images. Some of the known deep learning algorithms are stacked auto-encoders, deep Boltzmann machines, deep neural networks, and convolutional neural networks (CNNs). CNNs are the most commonly applied to image segmentation and classification. CNNs were first introduced in 1989 [12], but gained great interest after deep CNNs [1] achieved spectacular results in ImageNet competition in 2012. A typical CNN architecture contains subsequent layers of convolution, pooling, activation, and classification (fully connected).Convolutional layer produces feature maps by convolving a kernel across the input image. Pooling layer is used to down sample the output of preceding convolutional layers by using the maximum or average of the defined neighbourhood as the value passed to the next layer. Rectified Linear Unit (ReLU) and its modifications such as Leaky ReLU are among the most commonly used activation functions. ReLU nonlinearly transforms data by clipping any negative input values to zero while positive input values are passed as output [5].

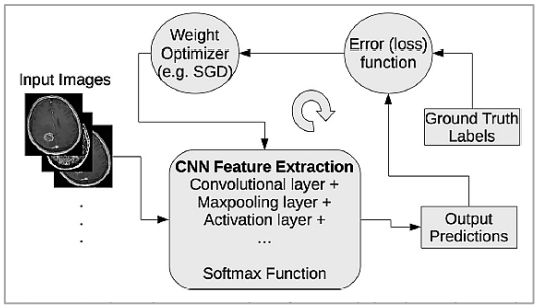

Figure 1.3: A schematic representation of a onvolutional neural network (CNN) training process.

2.1 Brain Region Segmentation using CNN

A fully automated system for brain region segmentation by using Human intelligence based deep learning technique is proposed. Deep learning technique is most popular state of the art method in recent applications. Figure. 5 shows the flow diagram of proposed methodology. There are two stages: pre-processing and segmentation via Convolutional Neural Network (CNN).The MRI image with noise is used as an input image. MRI images are collected from publicly available database Open Access Series of Image Studies (OASIS). Three layers are used in this network, which is used to segment the brain region.

A. Pre-processing: The MR images are first given to pre-processing step to enhance the quality of image for segmentation. In this work, Non Local Mean Filter is used for image de-noising which calculates weighted average of pixels and finding similarity with the target pixel. It consists of four steps.

Step 1: The weighted average non-local pixel is used to consider the data redundancy among the "patches" of the noisy image, and the noise free pixel is restored. The restored intensity, NL [u (x_i)] of the noisy pixel u (x_j) in the search window V_i is given by:

$$NL\,[u\,(x_i)] = \sum_{x_j \in v_j} w\,(x_i, x_j)\,u\,(x_j) \ldots\ldots\ldots\ldots\ldots\ldots\ldots (1)$$

Where, M is the radius of the search window V_i (x_i, x_j) is the weight allocate to the noisy value u $(x_j)$to establish the intensity at u (x_i) voxel x_i.

Step 2: The weight estimate the similarity between the intensity of the two neighbourhood patches Ni and Nj concentrate on voxels xi and xj is estimated by the weight such that w (x_i, x_j) $\in [0,1]$

Step 3: The weight based on the squared Euclidean distance between intensity patches u $(N_i)$and u (N_j) is gives as:

$$w\,(x_i, x_j) = \frac{1}{2}\exp\left(-\frac{\|u\,(N_i) - u\,(N_j)\|_2^2}{h^2}\right) \ldots\ldots\ldots (2)$$

Where, $\sum_{x_j \in v_j} w\,(x_i, x_j) = 1$ is ensured by the normalization constant, Zi is the variable for exponential decay control, h is given by, h = kσ where k is the smoothing parameter and σ is the noise standard deviation. By using Non Local Mean filter algorithm the noise is greatly reduced. It is an effective method to reduce the noise and it takes less time. One of the advantages of using Non Local Mean (NLM) filter is it does not loss any information from the input image.

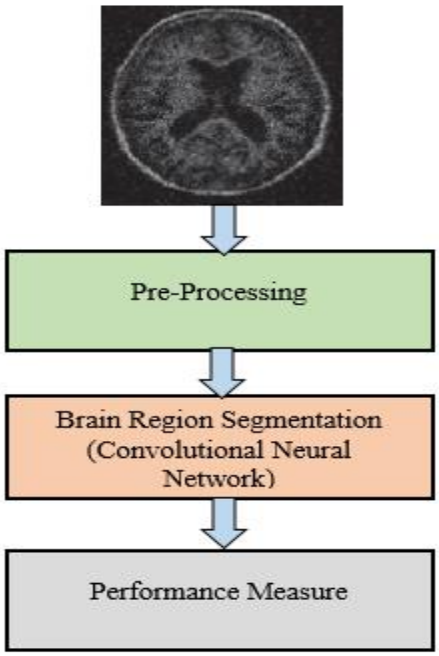

Figure 1.4: Flow Diagram of the used methodology

To perform a prediction of an input data, the output scores of the final CNN layer are connected to loss function (e.g., cross-entropy loss that normalizes scores into multinomial distribution over labels). Finally, parameters of the network are found by minimizing a loss function between prediction and ground truth labels with regularization constraints, and the network weights are updated a teach iteration (e.g., using stochastic gradient descent-SGD)using backpropagation until convergence as shown in figure 4.

1.4 CNN Architecture Styles

1. Patch-Wise CNN Architecture: This is a simple approach to train a CNN algorithm for segmentation. An NxN patch around each pixel is extracted from a given image, and the model is trained on these patches and given class labels to correctly identify classes such as normal brain and tumor. The designed networks contain multiple convolutional, activation, pooling, and fully connected layers sequentially.

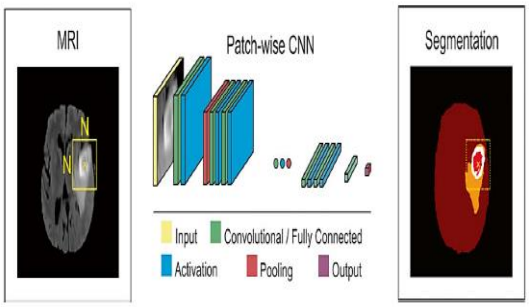

Figure 1.5: Schematic illustration of a patch-wise CNN architecture for brain tumor segmentation task [16].

2. Semantic-Wise CNN Architecture: This type of architecture makes predictions for each pixel of the whole input image like semantic segmentation [6] [9]. Similar to auto encoders, they include encoder part that extracts features and decoder part that up samples or de-convolves the higher level features from the encoder part and combines lower level features from the encoder part to classify pixels. The input image is mapped to the segmentation labels in a way that minimizes a loss function.

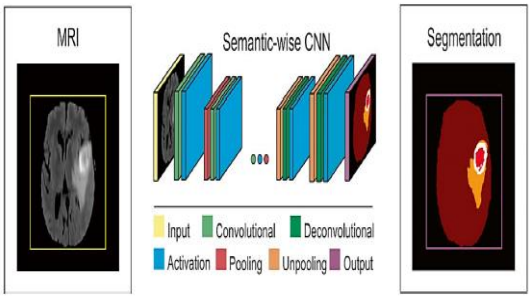

Figure 1.6: Schematic illustration of asemantic-wise CNN architecture for brain tumor segmentation task [16]

3. Cascaded CNN Architecture: This type of architecture combines two CNN architectures [7]. The output of the first CNN is used as an input to the second CNN to obtain classification results. The first CNN is used to train the model with initial prediction of class labels while second CNN is used to further tune the results of the first CNN.

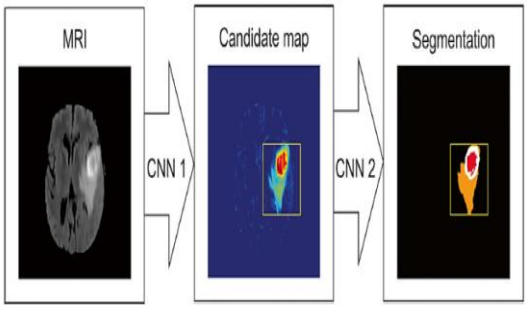

Figure 1.7 Schematic illustration of a cascaded CNN architecture for brain tumor segmentation

where the output of the first network (CNN 1) is used in addition to image data for are fined input to the second network (CNN2), which provides final segmentation [16]

II. RELATED WORK

Bao, S. et.al [1] proposed a novel method for brain MR image segmentation has been with deep learning techniques in order to obtain preliminary labelling and graphical models to produce the final result. A specific architecture, namely multi-scale structured convolutional neural networks (MS-CNN), is designed to capture discriminative features for each sub-cortical structure and to generate a label probability map for the target image**. Akkus, Z. et.al [3]** aims to provide an overview of current deep learning-based segmentation approaches for quantitative brain MRI. First we review the current deep learning architectures used for segmentation of anatomical brain structures and brain lesions. Next, the performance, speed, and properties of deep learning approaches are summarized and discussed. Finally, we provide a critical assessment of the current state and identify likely future developments and trends. After that **Havaei, M. et.al [4]** presented a fully automatic brain tumor segmentation method based on Deep Neural Networks (DNNs). The proposed networks are tailored to glioblastomas (both low and high grade) pictured in MR images. By their very nature, these tumors can appear anywhere in the brain and have almost any kind of shape, size, and contrast. These reasons motivate our exploration of a machine learning solution that exploits a flexible, high capacity DNN while being extremely efficient. **Akkus, Z. et.al [5]** predicted the 1p/19q status from MR images using convolutional neural networks (CNN), which could be a non-invasive alternative to surgical biopsy and histopathological analysis. Method: Our method consists of three main steps: image registration, tumor segmentation, and classification of 1p/19q status using CNN. The experts included a total of 159 LGG with 3 image slices each who had biopsy-proven 1p/19q status (57 non-deleted and 102 co-deleted) and preoperative postcontrast-T1 (T1C) and T2 images. The experts divided our data into training, validation, and test sets. The training data was balanced for equal class probability and then augmented with iterations of random translational shift, rotation, and horizontal and vertical flips to increase the size of the training set. Finally, the analysts evaluated several configurations of a multi-scale CNN architecture until training and validation accuracies became consistent. **Tom Brosch, et.al [6]** proposed a novel segmentation approach based on deep 3D convolutional encoder networks with shortcut connections and apply it to the segmentation of multiple sclerosis (MS) lesions in magnetic resonance images. The model consists of a neural network that consists of two interconnected pathways, a convolutional pathway, which learns increasingly more abstract and higher-level image features, and a de-convolutional pathway, which predicts the final segmentation at the voxel level. The researchers have evaluated our method on two publicly available data sets (MICCAI 2008 and ISBI 2015 challenges) with the results showing that our method performs comparably to the top-ranked state-of-the-art methods, even when only relatively small data sets are available for training. **Dou,Q. et.al [7]** proposed a novel automatic method to detect CMBs from magnetic resonance (MR) images by exploiting the 3D convolutional neural network (CNN). Compared with previous methods that employed either low-level hand-crafted descriptors or 2D CNNs, our method can take full advantage of spatial contextual information in MR volumes to extract more representative high-level features for CMBs, and hence achieve a much better detection accuracy. Then **Moeskops, P. et.al [8]** presents a method for the automatic segmentation of MR brain images into a number of tissue classes using a convolutional neural network. To ensure that the method obtains accurate segmentation details as well as spatial consistency, the network uses multiple patch sizes and multiple convolution kernel sizes to acquire multi-scale information about each voxel. The method is not dependent on explicit features, but learns to recognise the information that is important for the classification based on training data. The method requires a single anatomical MR image only. After That **Nie, D. et.al [9]** specifically conducted a convolution-pooling stream for multimodality information from T1, T2, and FA images separately, and then combine them in high-layer for finally generating the segmentation maps as the outputs. We compared the performance of our approach with that of the commonly used segmentation methods on a set of manually segmented isointense phase brain images. Results showed that our proposed model significantly outperformed previous methods in terms of accuracy. In addition, our results also indicated a better way of integrating multi-modality images, which leads to performance improvement. Xavier Then **Fernandez, T. et.al [10]** proposed a new algorithm that achieves lesion and brain tissue segmentation through simultaneous estimation of a spatially global within-the-subject intensity distribution and a spatially local intensity distribution derived from a healthy

reference population. The experts have demonstrated that MS lesions can be segmented as outliers from this intensity model of population and subject. They carried out extensive experiments with both synthetic and clinical data, and compared the performance of our new algorithm to those of state-of-the art techniques. **Znhang, W. et.al [11]** proposes to use deep convolutional neural networks (CNNs) for segmenting isointense stage brain tissues using multi-modality MR images. CNNs are a type of deep models in which trainable filters and local neighbourhood pooling operations are applied alternatingly on the raw input images, resulting in a hierarchy of increasingly complex features. Specifically, the researchers have used multi-modality information from T1, T2, and fractional anisotropy (FA) images as inputs and then generated the segmentation maps as outputs. The multiple intermediate layers applied convolution, pooling, normalization, and other operations to capture the highly nonlinear mappings between inputs and outputs. **Wang, L. et.al [12]** proposed a novel learning-based multi-source integration framework for segmentation of infant brain images. Specifically, the experts have employed the random forest technique to effectively integrate features from multi-source images together for tissue segmentation. Here, the multi-source images include initially only the multi-modality (T1, T2 and FA) images and later also the iteratively estimated and refined tissue probability maps of gray matter, white matter, and cerebrospinal fluid.Then **Maier, O. et.al [13]** presented nine classification methods (e.g. Generalized Linear Models, Random Decision Forests and Convolutional Neural Networks) are evaluated and compared with each other using 37 multi-parametric MRI datasets of ischemic stroke patients in the sub-acute phase in terms of their accuracy and reliability for ischemic stroke lesion segmentation. Within this context, a multi-spectral classification approach was compared against mono-spectral classification performance using only FLAIR MRI datasets and two sets of expert segmentations are used for inter-observer agreement evaluation. **Brebisson, A.D. et.al [14]** presented a novel approach to automatically segment magnetic resonance (MR) images of the human brain into anatomical regions. Our methodology was based on a deep artificial neural network that assigns each voxel in an MR image of the brain to its corresponding anatomical region. The inputs of the network capture information at different scales around the voxel of interest: 3D and orthogonal 2D intensity patches capture a local spatial context while large compressed 2D orthogonal patches and distances to the regional centroids enforce global spatial consistency.

III. THE PROPOSED METHOD

3.1 Proposed Framework

3.1.1 Convolution

Considering a network with $\tilde{L} \geq 1$. Among $\tilde{L}$ layers, $\tilde{L} - 1$ represent hidden type of layers. Let y_o represent the network input. For each of the layer $\tilde{I} \in \{1, 2, \ldots, \tilde{L}\}$ set $a_{\tilde{I}} = \omega_{\tilde{I}} s\,(a_{\tilde{I}-1})$ where s presents a vector-based function, $s(a_0) = x_0$. The layers of consecutive nature are interlinked. Let $f(\omega, x_0)$ and $\omega = (\omega_{\tilde{I}})_{\tilde{I}}$ be the network output at end of $\tilde{L}$th layers.

1. Local gradient based back propagated error: Each of the layer $\tilde{I}$ involves various units. The local gradient based back propagated error is usually defined by $(El)_{a_i}$ as the partial derivative at ith unit: The use of rule based on classical chain results in:

$$(El)_{a_i} = (El)_{a_j} \cdot (a_j)_{wij}$$

2. Linear Networks: We usually refer to the network of linear form when there is "s" type of mapping which identifies the function; s (a) = a: In such type of case, the $f(\omega, x_0)$ output function represents a weight-based polynomial function.

3. Maxout: This layer represents a simple layer where the activation-based function is the maxima of inputs.

4. Maxpooling: It is usually done by putting into use of a maximized filter to sub regions (non-overlapping) of the primary representation as shown in figure 3.1 below.

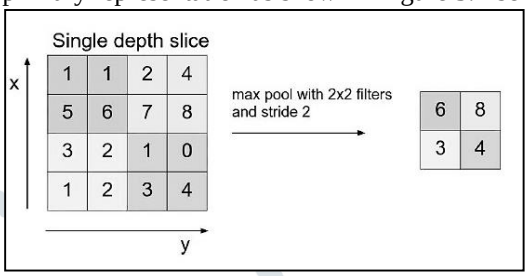

Figure 3.1: Maxpool operation example

A unit of max-pooling 'j' outputs the maxima of all the unit outputs from where it accepts the inputs. Further to the process of max pooling, the units of pooling can perform various other type of functions like L2-norm pooling or even the process of average pooling.

5. Rectifiers: This represents a neuron layer that is applies the activation function of non-saturating form $s(a) = \max(0; a)$: The other type of functions are mainly used for increasing the nonlinearity, for instance, the saturating form of hyperbolic tangent $s(a) = \tanh(a)$; $s(a) = j\tanh(a)j$, and $s(a) = (1 + e^{-\alpha})^{-1}$as the sigmoid function: The RLU i.e. Rectified Linear Units are mainly used in various kind of implementations.

6. Dropout: The technique of dropout helps in improving the neural networks and basically aims to mitigate or reduce the overfitting problem. It mainly comprises of dropping out all the units (visible and hidden) in the methodology of neural networks. With this technology, it usually ignores all the operations of that specific units, along with its outgoing and incoming links or connections.

7. Dropconnect: It represents dropout refinement where instead of units, the links are dropped during the period of training.

8. Convolution layers: In a convolutional layer, the units of convolutional layer shares weight through a discrete type of convolution.

3.1.2 Learning the Network

Neural network learning presents a supervised (controlled) method of classification using a set of data as an unlabeled or unmanaged object as an investment (input). Data collection is mainly divided into three of the following parts, known as Authentication Kit, Test Kit, and Training Collection. The set of training is mainly used to prepare or train the network in the periods referred to as epochs/eras, during this process the loss function calculates two significant values i.e. accuracy and loss. These values show the accuracy and the error created by the network. The network for improving the design creates correct mapping of output/ input, even in case if the input is little distinct from the instances used in the phase of training. If the system network is well-trained, we are risking too much adaptation of the training collection data as the network learns the data-base noise present in it. This phenomenon is known as overfitting. The over-trained (prevailing) network

is extremely tough and therefore loses its extensions. To prevent this issue, the so-called "early termination/stopping" method is used. Learning the set of training is usually carried out until the era when the value of the loss for the set of validation begins to boost, the moment over which the overfitting effect begins [39]. After completion of the learning phase, the capability of classification of the network is further evaluated based on the operational cost of the loss calculated for the test package.

3.2 Proposed methodology: Flowchart

Step1: Input Brain MRI images.
Step 2: Pre-processed the image and denoise it.
Step 3: Next step is to extract the group of same area.
Step 4: Apply the convolution process.
Step 4: After Convolution extract the low level features and grouped them.
Step 5: Then check the output if it is optimized then jumps to step 6 otherwise go to step 4.
Step 6: Find the non-overlapping features and then analyse PSNR, MSE and Accuracy.

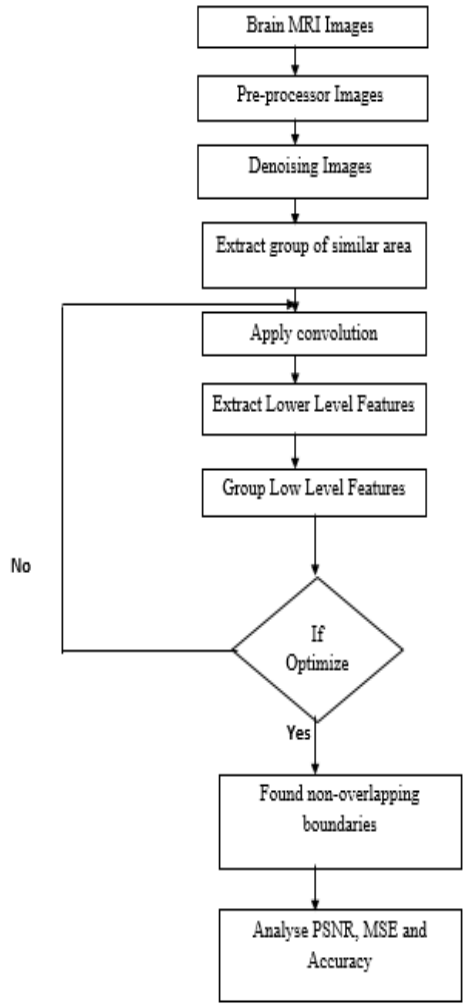

Figure 3.2: Proposed Flowchart

3.3 Algorithm Used

1. Particle Swarm Optimization (PSO): is an optimization technique that is based upon bird flocking and fish schooling. Swarm is the collection of particles. There is some objective function whose value has to be optimized with PSO. The optimized value of the objective function will be some point in the search space. Every particle moves in the search space to find the point at which objective function is optimized. At any point of time, every particle has some position and velocity in the search space. Initially, positions and velocities of particles are randomly assigned. After each iteration, positions and velocities of particles are updated using equations 1 and 2. Every particle in PSO has its local best position and the global best position of the swarm. Global best position of the swarm is the position of the particle which is more close to the optimal value. All the particles will move towards the global best position as it is close to the optimal value.

$V_{i,d}(t+1) = \alpha(t)V_{i,d}(t) + \beta pranp(t)(persbesti,d - P_{i,d}(t)) + \beta grang(t)(globestd - P_{i,d}(t))$……..(1)

$P_{i,d}(t+1) = P_{i,d}(t) + V_{i,d}(t)$……(2)

Where $V_{i,d}$ and $P_{i,d}$ is the velocity and position of particle I , dimension d at iteration t+1.α(t) is the weight that tracks the history of velocity, βpranp(t) and βgrang(t) are the random factors,persbesti,d is the Personal Best of particle I for dimension d and globest is the Global Best of the swarm for dimension d.

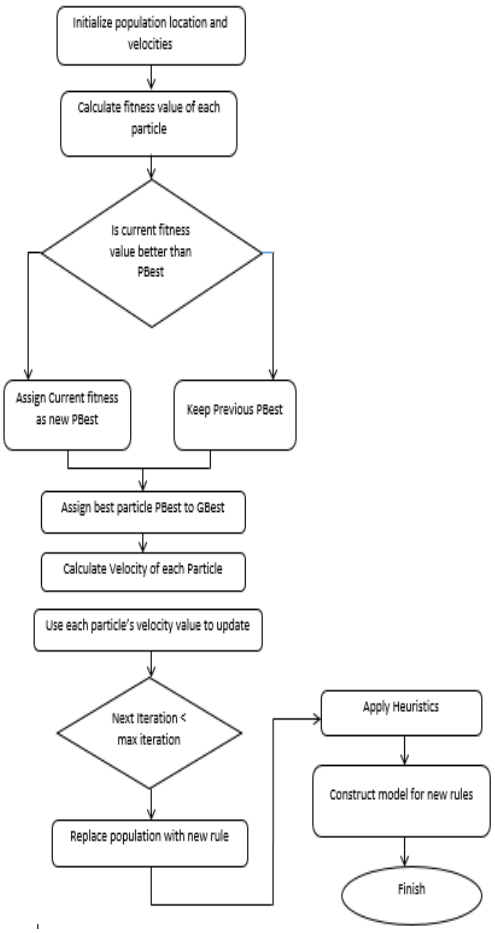

Figure 3.3: Flow Chart of PSO

PSO

Step 1: In PSO model for each particle i in S do
Step 2: for each dimension d in D do
Step 3: //initialize each particle's position and velocity
Step 4: $x_{i,d} = \boldsymbol{Rnd}(\boldsymbol{x_{max}}, \boldsymbol{x}_{\min})$
Step 5: $\boldsymbol{v_{i,d}} = \boldsymbol{Rnd}(-\boldsymbol{v_{max}}/3, \boldsymbol{v_{max}}/3)$
Step 6: end for
Step 7: //initialize particle's best position and velocity

$$\boldsymbol{v_i}(k+1) = \boldsymbol{v_i}(k) + \boldsymbol{\gamma 1_i}(\boldsymbol{p_i} - \boldsymbol{x_i}(k)) + \boldsymbol{\gamma_{2i}}(G - \boldsymbol{x_i}(k))$$

New velocity

$$\boldsymbol{x_i}(k+1) = \boldsymbol{x_i}(k) + \boldsymbol{v_i}(k+1)$$

Where
i- particle index
k- discrete time index
v_i –velocity of i^{th} particle
x_i – position of i^{th} particle
p_i- best position found by i^{th} particle(personal best)
G- best position found by swarm (global best, best of personal bests)
$G_{(1,2)i}$- random number on the interval[0,1]applied

to the i[th] particle
Step 8: $pb_i = x_i$
Step 9: // update global best position
Step10: if $f(pb_i) < f(gb)$
Step 11: $gb = pb_i$
Step12: end if
Step13: end for

IV. RESULT ANALYSIS

4.1 Platform Used

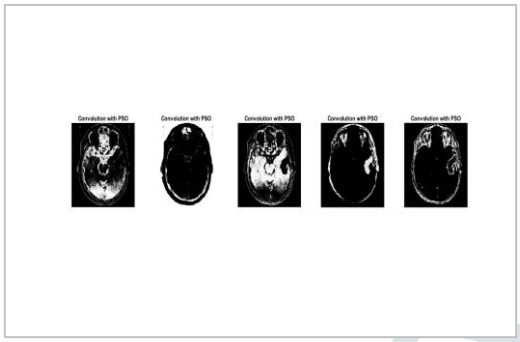

Figure 4.1: Different steps of image segmentation in proposed (convolution-PSO) approach

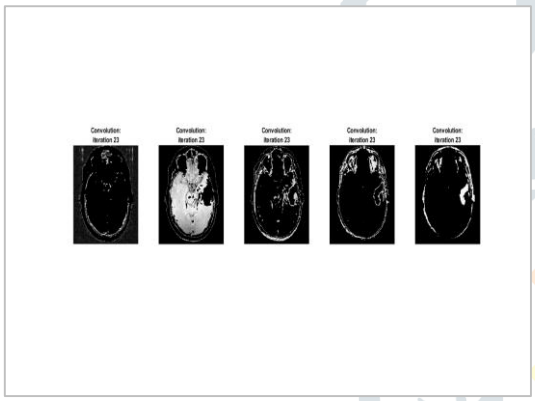

Figure 4.2: Different steps of image segmentation in Existing (convolution) approach

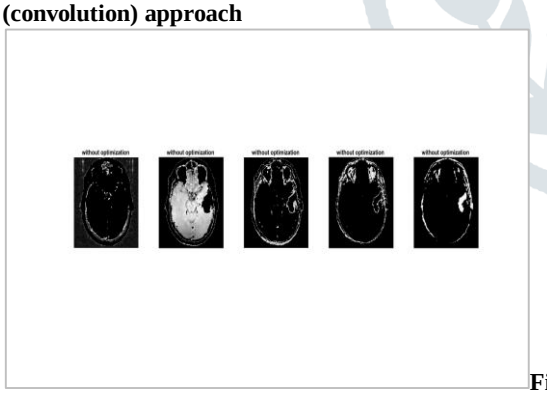

Figure 4.3: Different steps of image segmentation in Existing (without-optimization) approach

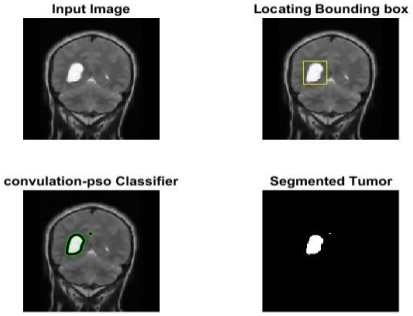

Figure 4.4: Different steps of image Classification in proposed (convolution-PSO) approach

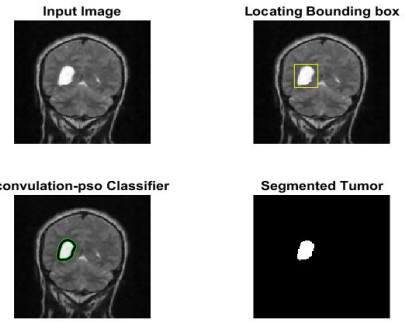

Figure 4.5: Different steps of image classification in proposed (convolution-PSO) approach

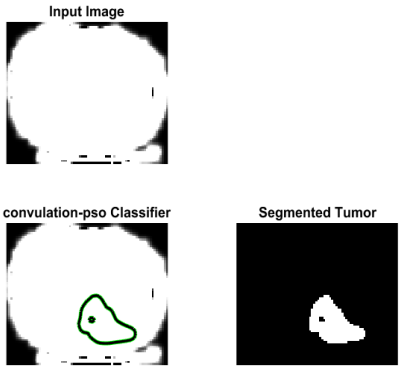

Figure 4.6: Different steps of image segmentation in Existing (convolution) approach.

Table 4.1: Comparison of PSNR between existing and proposed approach

Images	PSNR without optimization	PSNR-Convolution	PSNR-Convolution-PSO
Image1	21.78	22.34	26.56
Image2	22.62	24.34	27.45
Image3	23.12	25.35	27.45
Image4	20.34	21.45	22.44
Image5	21.34	24.34	25.35
Image6	26.45	27.45	29.45
Image7	29.45	32.45	33.45
Image8	30.45	34.34	36.33
Image9	32.45	33.244	34.34

Table 4.1 explains the comparison of PSNR between the proposed and the existing approaches. Here, PSNR represents the ratio between the maximized possible signal power and the power of corrupting noise that disturbs the reliability of its depiction. The value of PSNR (without optimization) has more corrupting noise and less signal power. But with PSNR (convolution), the value of corrupting noise reduces and the signal power is increased. Further, with PSNR (Convolution-PSO), the signal power improves more and corrupting noise reduces further. For PSNR to be maximum, the corrupting noise should be less and the signal power should be more.

i.e. $\text{PSNR} = \frac{\text{Max.possible signal power}}{\text{Power of corrupting noise}}$

For example take the results of Image 1, the value gets improved for the case of convolution and it is further improved using the mechanism of Convolution-PSO approach.

PSNR (without optimization) = 21.78
PSNR (Convolution) = 22.34
PSNR (Convolution-PSO) = 26.56

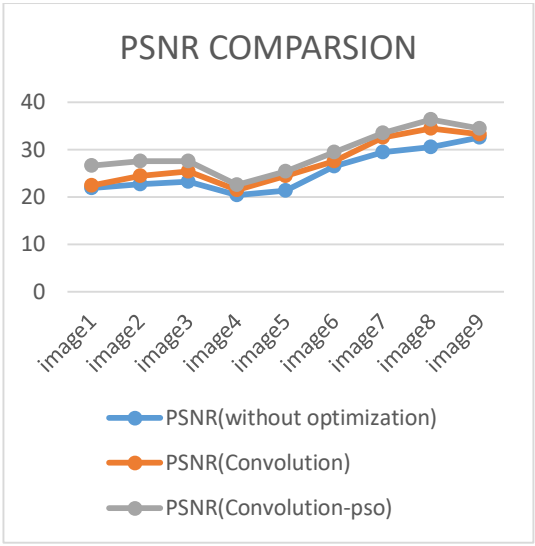

Figure 4.7: Graphical representations of PSNR comparison between Proposed and Existing approaches.

Figure 4.7 represents the graphical comparison of PSNR between the proposed and the existing approaches as per table 1 explained above.

Table 4.2: Comparison of Sensitivity between existing and proposed approach

Images	Sensitivity without optimization	Sensitivity Convolution	Sensitivity Convolution PSO
Image1	97.45	98.34	99.45
Image2	96.34	97	98.45
Image3	92.34	94.34	96.45
Image4	90.23	92.12	95.35
Image5	89.45	90.34	95.43

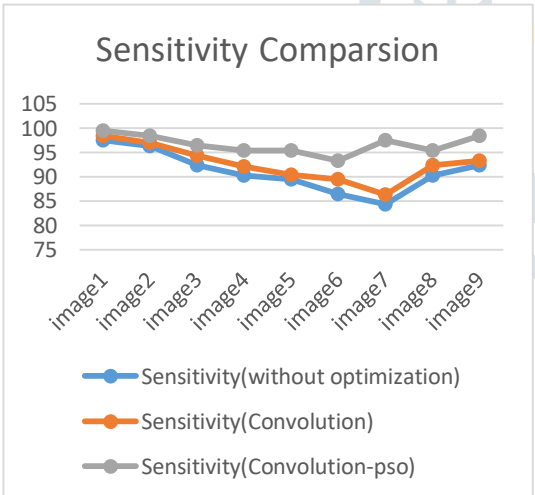

Image6	86.45	89.45	93.23
Image7	84.34	86.34	97.45
Image8	90.23	92.34	95.32
Image9	92.34	93.23	98.34

It represents the study that how the uncertainty in the output of a system can be distributed and assigned to diverse sources of uncertainty in its inputs. It is also called as true positive rate or the probability of detection. In terms of medical field, it measure the actual positive or present proportion of a disease that are appropriately recognized. For instance, the sick people percentage who are appropriately recognized to have that particular condition of suffering. For example take the results of Image 1, the value of sensitivity gets improved for the case of convolution and it is further improved using the mechanism of convolution-PSO approach. Sensitivity (without optimization) = 97.45

Sensitivity (Convolution) = 98.34

Sensitivity (Convolution-PSO) = 99.45

Figure 4.8: Graphical representations of Sensitivity comparison between proposed and existing approaches.

Figure 4.8 represents the graphical comparison of sensitivity between the proposed and the existing approaches as per table 4.2 explained above.

Table 4.3: Comparison of Specificity between existing and proposed approach

Images	Specificity without optimization	Specificity Convolution	Specificity Convolution PSO
Image1	96.895	97.67	98.95
Image2	94.34	95.67	97.45
Image3	91.285	93.23	95.9
Image4	89.84	91.23	95.39
Image5	87.95	89.895	94.33
Image6	85.395	87.895	95.34
Image7	87.285	89.34	96.385
Image8	91.285	92.785	96.83
Image9	92.34	93.23	98.34

It is also called as true negative rate or the probability of detection. In terms of medical field, it measure the actual negative or absent proportion of a disease that are appropriately recognized. For instance, the healthy people percentage who are appropriately recognized not to have that particular condition of suffering.

For example take the results of Image 1, the value of specificity gets improved for the case of convolution and it is further improved using the mechanism of convolution-PSO approach. Specificity (without optimization) = 96.895

Specificity (Convolution) = 97.67

Specificity (Convolution-PSO) = 98.95

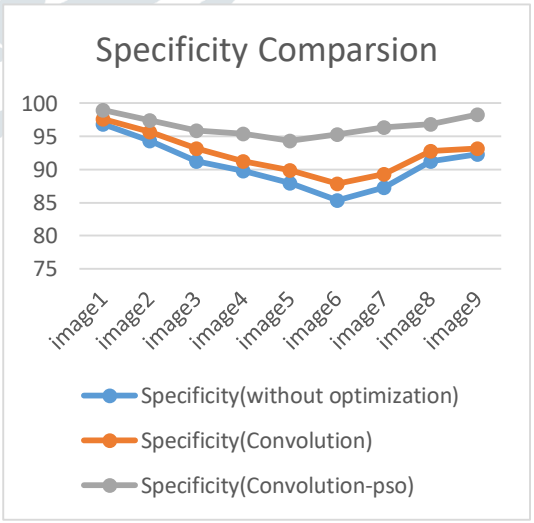

Figure 4.9: Graphical representations of Specificity comparison between proposed and existing approaches.

Figure 4.9 represents the graphical comparison of Specificity between the proposed and the existing approaches as per Table 4.3 explained above.

Table 4.4 Comparison of Accuracy between existing and proposed approach

Images	Accuracy without optimization	Accuracy Convolution	Accuracy Convolution -PSO
Image1	94.1733333	95.5233333	97.4333333
Image2	91.8216666	93.3766666	96.2466666
Image3	89.6916666	91.4516666	95.2066666
Image4	87.7283333	89.6733333	95.02
Image5	86.8766666	89.0433333	95.3516666
Image6	87.9883333	90.0066666	96.185
Image7	90.3033333	91.785	97.185
Image8	91.8125	93.0075	97.585
Image9	92.34	93.23	98.34

Table 4..4 presents the depiction of systematic errors, and a quantity of arithmetic bias.

For example take the results of Image 1, the value of accuracy gets improved for the case of convolution and it is further improved using the mechanism of convolution-PSO approach. Same happens for other cases taken in the above mentioned table 4.4

Accuracy (without optimization) = 94.17333333

Accuracy (Convolution) = 95.52333333

Accuracy (Convolution-PSO) = 97.43333333

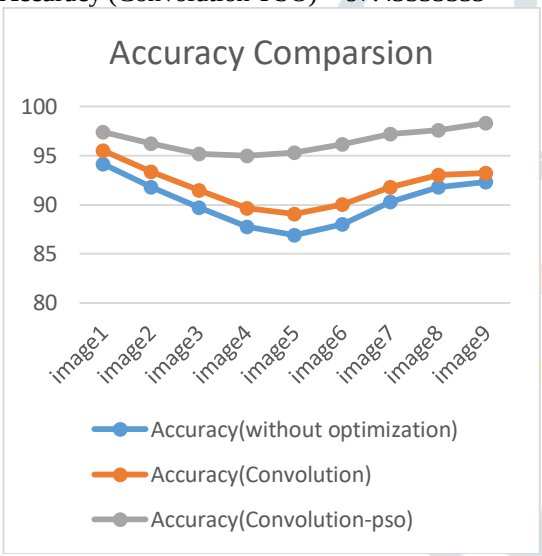

Figure 4.10: Graphical representations of Accuracy comparison between proposed and existing approaches

IV CONCLUSION

Brain tumor segmentation in magnetic resonance imaging (MRI) is considered a complex procedure because of the variability of tumor shapes and the complexity of determining the tumor location, size, and texture. Manual tumor segmentation is a time-consuming task highly prone to human error. Hence, this study proposes an automated method that can identify tumor slices and segment the tumor across all image slices in volumetric MRI brain scans. First, a set of algorithms in the pre-processing stage is used to clean and standardize the collected data. Brain tumor segmentation algorithms have relatively good results in the field of medical image analysis, there is a certain distance in clinical applications. Due to a lack of interaction between researchers and clinicians, clinicians still rely on manual segmentation for brain tumor in many cases. The existence of many tools aims to do pure research and is hardly useful for clinicians. Therefore, embedding the developed tools into more user friendly environments will become inevitable in the future. Recently, some standard clinical acquisition protocols focusing on feasibility studies are trying to formulate to improve the clinical applications more quickly. Apart from the evaluation of accuracy and validity for the results of brain tumor segmentation, computation time is also an important criterion. The current standard computation time is in general a few minutes. The real-time segmentation will be hard to achieve, but computation time over a few minutes is unacceptable in clinical routine. Another crucial aspect for brain tumor segmentation methods is robustness. If an automatic segmentation technique fails in some cases, clinicians will lose their trust and not use this technique. Therefore, the robustness is also one of the major assessment criteria for each new method applied in clinical practice. Some current brain tumor segmentation methods provide robust results within a reasonable computation time. In proposed approach select the optimize block from convolution process which improve the accuracy sensitivity, specificity and accuracy.

V REFERENCES

[1] Bao, S., & Chung, A. C. (2018). Multi-scale structured CNN with label consistency for brain MR image segmentation. Computer Methods in Biomechanics and Biomedical Engineering: Imaging & Visualization, 6(1), 113-117.

[2] Kamnitsas, K., Ledig, C., Newcombe, V. F., Simpson, J. P., Kane, A. D., Menon, D. K., & Glocker, B. (2017). Efficient multi-scale 3D CNN with fully connected CRF for accurate brain lesion segmentation. Medical image analysis, 36, 61-78.

[3] Akkus, Z., Galimzianova, A., Hoogi, A., Rubin, D. L., & Erickson, B. J. (2017). Deep learning for brain MRI segmentation: state of the art and future directions. Journal of digital imaging, 30(4), 449-459.

[4] Havaei, M., Davy, A., Warde-Farley, D., Biard, A., Courville, A., Bengio, Y., & Larochelle, H. (2017). Brain tumor segmentation with deep neural networks. Medical image analysis, 35, 18-31.

[5] Akkus, Z., Ali, I., Sedlář, J., Kline, T. L., Agrawal, J. P., & Parney, I. F. Predicting 1p19q Chromosomal Deletion of Low-Grade Gliomas from MR Images Using Deep Learning.(2016).

[6] Brosch, T., Tang, L. Y., Yoo, Y., Li, D. K., Traboulsee, A., & Tam, R. (2016). Deep 3D convolutional encoder networks with shortcuts for multiscale feature integration applied to multiple sclerosis lesion segmentation. IEEE transactions on medical imaging, 35(5), 1229-1239.

[7] Dou, Q., Chen, H., Yu, L., Zhao, L., Qin, J., Wang, D., & Heng, P. A. (2016). Automatic detection of cerebral microbleeds from MR images via 3D convolutional neural networks. IEEE transactions on medical imaging, 35(5), 1182-1195.

[8]. Moeskops, P., Viergever, M. A., Mendrik, A. M., de Vries, L. S., Benders, M. J., & Išgum, I. (2016). Automatic segmentation of MR brain images with a convolutional neural network. IEEE transactions on medical imaging, 35(5), 1252-1261.

[9] Nie, D., Wang, L., Gao, Y., & Sken, D. (2016, April). Fully convolutional networks for multi-modality isointense infant brain image segmentation. In 2016 IEEE 13th International Symposium on Biomedical Imaging (ISBI) (pp. 1342-1345). IEEE.

[10] Tomas-Fernandez, X., & Warfield, S. K. (2015). A model of population and subject (MOPS) intensities with application to multiple sclerosis lesion segmentation. IEEE transactions on medical imaging, 34(6), 1349-1361.

[11] Zhang, W., Li, R., Deng, H., Wang, L., Lin, W., Ji, S., & Shen, D. (2015). Deep convolutional neural networks for

multi-modality isointense infant brain image segmentation. NeuroImage, 108, 214-224.
[12] Wang, L., Gao, Y., Shi, F., Li, G., Gilmore, J. H., Lin, W., & Shen, D. (2015). LINKS: Learning-based multi-source IntegratioN frameworK for Segmentation of infant brain images. NeuroImage, 108, 160-172.
[13] Maier, O., Schröder, C., Forkert, N. D., Martinetz, T., & Handels, H. (2015). Classifiers for ischemic stroke lesion segmentation: a comparison study. PloS one, 10(12), e0145118.
[14] de Brebisson, A., & Montana, G. (2015). Deep neural networks for anatomical brain segmentation. In Proceedings of the IEEE Conference on Computer Vision and Pattern Recognition Workshops (pp. 20-28).
[15] Weiss, N., Rueckert, D., & Rao, A. (2013, September). Multiple sclerosis lesion segmentation using dictionary learning and sparse coding. In International Conference on Medical Image Computing and Computer-Assisted Intervention (pp. 735-742). Springer, Berlin, Heidelberg.
[16] Senthilkumaran, N., & Rajesh, R. (2011). Brain image segmentation. International journal of wisdom based computing, 1(3), 14-18.
[17] Gudmundsson, M., El-Kwae, E. A., & Kabuka, M. R. (1998). Edge detection in medical images using a genetic algorithm. IEEE transactions on medical imaging, 17(3), 469-474.
[18] LeCun, Y., Boser, B., Denker, J. S., Henderson, D., Howard, R. E., Hubbard, W., & Jackel, L. D. (1989). Backpropagation applied to handwritten zip code recognition. Neural computation, 1(4), 541-551.